

KINETIC STUDIES LINKING THE TRIPHOSPHOINOSITIDE EFFECT TO  
MUSCARINIC RECEPTOR ACTIVATION AND THE CONTRACTION  
RESPONSE IN RABBIT IRIS MUSCLE

by

Marilyn Jean Grimes

Submitted to the Faculty of the School of Graduate Studies  
of the Medical College of Georgia in Partial Fulfillment  
of the Requirements for the Degree of  
Master of Science

May

1979

119522

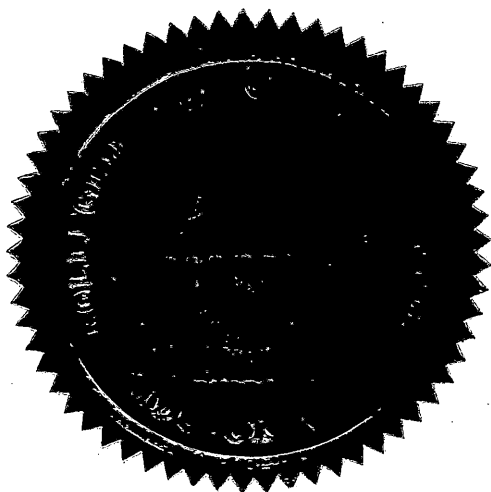
Kinetic Studies Linking the Triphosphoinositide Effect to  
Muscarinic Receptor Activation and the Contraction  
Response in Rabbit Iris Muscle

This thesis submitted by Marilyn Jean Grimes has been examined and approved by an appointed committee of the faculty of the School of Graduate Studies of the Medical College of Georgia.

The signatures which appear below verify the fact that all required changes have been incorporated and that the thesis has received final approval with reference to content, form and accuracy of presentation.

This thesis is therefore accepted in partial fulfillment of the requirements for the degree of Master of Science.

June 4, 1979  
Date



[Redacted signature]

Advisor

[Redacted signature]

Chairman, Department of Cell and  
Molecular Biology

[Redacted signature]

Dean, School of Graduate Studies

#### ACKNOWLEDGMENTS

I am sincerely grateful to my advisor, Dr. A.A. Abdel-Latif, for his guidance throughout this project. I also thank Dr. G. Carrier for his invaluable assistance on the contraction studies. Special thanks are given to my co-workers, Rashid and Jack, for their never-ending encouragement.

## TABLE OF CONTENTS

	Page
INTRODUCTION	
I. Review of the Related Literature	1
II. Statement of Problem	6
MATERIALS AND METHODS	
I. Materials	
A. Radioactive and Non-Radioactive Compounds	8
B. Animals	8
II. Methods	
A. Determination of Dose-Triphosphoinositide (TPI) and Dose-Phosphatidic Acid (PA) Responses	8
1. Preparation of irises	8
2. Incubation of irises	8
3. Extraction of phospholipids	9
4. Isolation of lipids by thin-layer chromatography (TLC)	10
5. Measurement of phospholipid radioactivity	12
6. Construction of dose-TPI and dose-PA response curves	12
B. Determination of Dose-Tension Responses	13
1. Preparation of the irises	13
2. Incubation of irises	13
3. Determination of the contraction response	14
4. Construction of dose-contraction response curves	15
C. Calculations and Determinations of the Kinetic Constants from the TPI, PA, and Contraction Data	15
RESULTS	
I. Effect of Incubation Time on the $^{32}\text{P}$ -Radioactivity of TPI and PA After Addition of ACh	17
II. Dose-Response Curves (TPI-Breakdown, PA-Labeling, and Contraction Responses) to Various Muscarinic Agonists	17
III. Dose-Response Curves (TPI-Breakdown, PA-Labeling, and Contraction Responses) to ACh in the Presence and Absence of Atropine and Measurement of Atropine Antagonism	19
DISCUSSION	33
SUMMARY	39
REFERENCES	41

# LIST OF FIGURES

Figure	Page
1. <i>Scheme showing the possible role for the TPI effect at the postsynaptic membrane of the iris smooth muscle</i>	5
2. <i>Separation of iris muscle phospholipids by means of two-dimensional t.l.c.</i>	11
3. <i>Effect of acetylcholine (ACh), at various time intervals, on tissue phospholipids</i>	18
4. <i>Dose-response curves (TPI-breakdown) to ACh, acetyl-<math>\beta</math>-methacholine, and carbachol in rabbit iris muscle</i>	20
5. <i>Dose-response curves (PA-labelling) to ACh, acetyl-<math>\beta</math>-methacholine, and carbachol in rabbit iris muscle</i>	21
6. <i>Dose-response curves (contraction) to ACh, acetyl-<math>\beta</math>-methacholine, and carbachol in rabbit iris muscle</i>	22
7. <i>Dose-response curves (TPI-breakdown) to ACh in the absence and presence of atropine in the rabbit iris muscle</i>	25
8. <i>Dose-response curves (PA-labelling) to ACh in the absence and presence of atropine in the rabbit iris muscle</i>	26
9. <i>Dose-response curves (contraction) to ACh in the absence and presence of atropine in rabbit iris muscle</i>	27
10. <i>Arunlakshana-Schild plot based on the dose-response curves for ACh and atropine with the TPI response (see Fig. 7)</i>	29
11. <i>Arunlakshana-Schild plot based on the dose-response curves for ACh and atropine with the PA response (see Fig. 8)</i>	30
12. <i>Arunlakshana-Schild plot for the dose-response curves to ACh and atropine for the contraction response (see Fig. 9)</i>	31

## LIST OF TABLES

Table	Page
1. <i>Relative affinities (<math>-\log ED_{50}</math>) of cholinergic agonists for iris muscle muscarinic receptors obtained from the biochemical and pharmacological methods</i>	23
2. <i>Dissociation constants for the atropine-muscarinic receptor complex obtained from the biochemical and pharmacological methods</i>	32
3. <i>Comparison of kinetic constants derived from binding, contraction, and biochemical responses in smooth muscle</i>	35

## INTRODUCTION

### I. Review of Related Literature:

Since the various functional properties of biomembranes are known to be related to their physicochemical characteristics, any information related to their composition and turnover appears to be helpful to understanding the relationship between structure and function. Membranes play such crucial roles as: maintenance of the internal composition of a cell, packaging and translocation of macromolecules, and transmission of extracellular information to the cell interior. Involvement of inositol lipids in these membrane functions has been suggested by a variety of observations (28).

Several workers have suggested that the interconversion of triphosphoinositide (TPI) and diphosphoinositide (DPI) may be responsible for the changes in  $\text{Na}^+$  and  $\text{K}^+$  permeability of neuronal membranes. For instance, Kai and Hawthorne (27) proposed a model in which polyphosphoinositides and their enzymes were involved in the permeability changes associated with excitation. They suggested that the dephosphorylation of polyphosphoinositides in the nerve axonal membrane results in a release of bound  $\text{Ca}^{++}$  ions which opens pores with increased permeability to monovalent ions by affecting polyphosphoinositide-protein complexes in the membrane. Durell and co-workers proposed a theory that ACh induced depolarization at the synapse in neural tissue through an effect on the rate of phosphodiesteratic cleavage of one or more of the phosphoinositides (15). Preliminary experimental evidence from

Durell's laboratory suggested that this effect of ACh on the hydrolysis of the phosphoinositides may be the primary effect leading to secondary increases in synthesis of phospholipids, particularly phosphatidic acid (PA) and phosphatidylinositol (PI).

Investigations attempting to define the functional role of increased polyphosphoinositide turnover in response to external stimuli have resulted in confusing and often contradictory experimental results in various tissues. For instance, attempts in the past by several investigators to alter the labeling of DPI and TPI by ACh have produced no significant changes in such tissues as sympathetic or vagal ganglia (26), synaptosomes (39), and brain (31). On the other hand, Birnberger *et al.* (10) have shown that after incubations of 60 min and brief electrical stimulation (5 min) there is an increased turnover of TPI in lobster nerves. Schacht and Agranoff (33) observed a decreased labeling of the polyphosphoinositides with  $^{32}\text{P}$  in guinea pig brain-cortex subfractions incubated with ACh. In 1973, White and Larrabee (37) reported a specific reduction in the labeling of TPI in rat vagus nerve after electrical stimulation for three hours. More recently, White *et al.* (38) noted that stimulation of vagus nerve for 30 min increased the phosphate incorporation into all the phospholipids studied, but the increase was significant only in the phospholipids TPI and DPI.

Hendrickson and Reinertsen (24) have reported results from experiments comparing the ion affinities of DPI and TPI. Their measurements were actually made with the water-soluble deacylation products derived



from DPI and TPI, but results were extrapolated back to the lipids themselves. They concluded that TPI had considerably higher affinity for  $\text{Ca}^{++}$  than DPI, presumably because it could use the two phosphate groups on the inositol ring to form a chelate with divalent metal ions. They proposed that the TPI/DPI interconversion might itself be adequate to markedly modify  $\text{Ca}^{++}$ -binding to membrane surfaces and also to control intracellular concentrations of  $\text{Ca}^{++}$ . They set up an hypothetical method of axonal membrane function and clearly demonstrated that the amount of  $\text{Ca}^{++}$  bound to inositides and, presumably, to membranes containing them could indeed be markedly lowered by TPI  $\rightarrow$  DPI conversion in their scheme. They proposed that these changes could conceivably cause a reorganization of the membrane with a resulting change in  $\text{Na}^+$  and  $\text{K}^+$  permeability (25).

Torda (35) proposed a mechanism for the fast generation of action potentials at cholinergic nicotinic synapses. She suggested that activation of TPI-phosphomonoesterase by ACh may be one of the molecular mechanisms which couple the formation of ACh-receptor complex to the depolarization of the postsynaptic membrane.

Recent communications from Cho and co-workers (14) presented findings which suggested the possibility that TPI is a binding site of the nicotinic receptor. Their experimental evidence showed that TPI binds nicotinic agonists and antagonists with high affinities, and the dissociation constants obtained were comparable to those reported for the same agents binding to purified nicotinic receptor. Furthermore, they have

shown that upon addition of  $1 \times 10^{-4}$  M  $\text{CaCl}_2$  to their incubation medium, the binding of various nicotinic agonists was enhanced; it is well known that calcium ions increase the binding of cholinergic ligands to their receptors (12b).

Communications from Abdel-Latif's laboratory have reported that stimulation of cholinergic muscarinic and alpha-adrenergic receptors in iris smooth muscle provoke TPI breakdown and that these effects are blocked by atropine and phentolamine, respectively (1). This phenomenon has been termed the "TPI Effect". More recent work has indicated that this phenomenon is mediated by  $\text{Ca}^{++}$  (7). This finding showed that the ACh-stimulated breakdown of TPI and labeling of PA were dependent upon the presence of extracellular  $\text{Ca}^{++}$ ; it is possible that a transmembrane flux of  $\text{Ca}^{++}$  was required for the TPI Effect to occur. There were several lines of evidence which suggested that activation of cholinergic muscarinic receptors led to increased influx of  $\text{Ca}^{++}$  in several tissues (13,34) including the iris muscle (7).

A scheme, based in part on the work of Abdel-Latif *et al.*, was recently proposed showing the possible role of TPI and its enzymes at cholinergic muscarinic and  $\alpha$ -adrenergic receptors (Fig. 1). The essential features of the sequence of events are as follows: 1) The interaction between the neurotransmitter and its receptor leads to elevation of intracellular  $\text{Ca}^{++}$  (7). 2) This  $\text{Ca}^{++}$ , in turn, stimulates the breakdown of TPI which could result in changes in membrane structure. The enzyme involved in this neurotransmitter-stimulated breakdown of TPI is TPI-phosphodiesterase, which is activated by  $\text{Ca}^{++}$  (6).

Figure 1. *Scheme showing the possible role for the TPI effect at the postsynaptic membrane of the iris smooth muscle.*

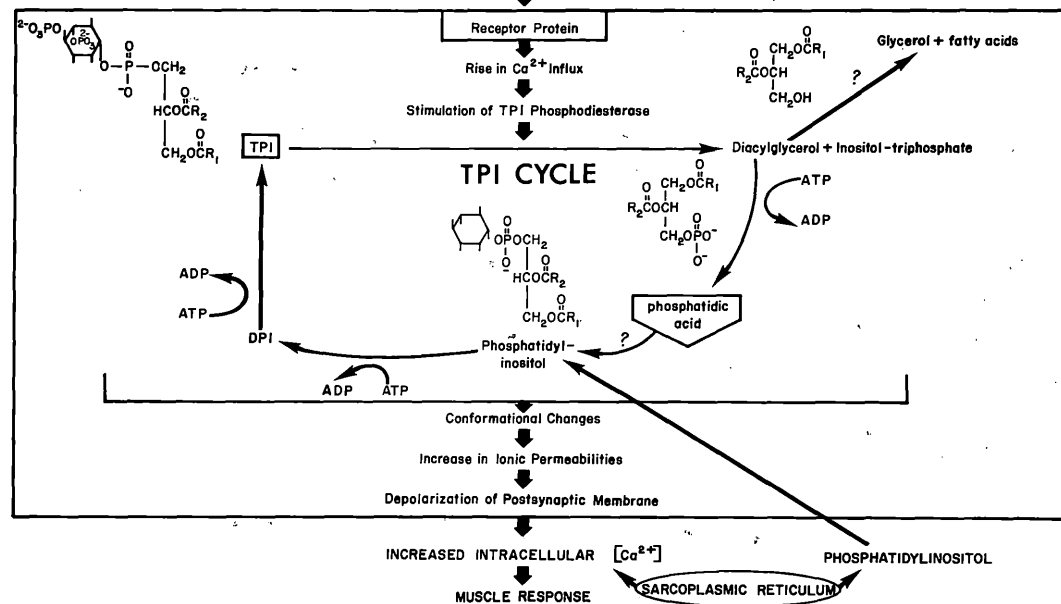
The essential features of the sequence of events are as follows: 1) Neurotransmitter-receptor interaction leads to  $\text{Ca}^{++}$  elevation; 2)  $\text{Ca}^{++}$  stimulates the breakdown of TPI which could result in changes in membrane structure; and 3) changes in membrane structure caused by TPI breakdown could lead to changes in  $\text{Na}^+$ ,  $\text{K}^+$  permeability and subsequently muscle contraction (based in part on previous studies with rabbit iris muscle (4,7); A.A. Abdel-Latif, unpublished work).

EXTRACELLULAR

$\alpha$ -ADRENERGIC OR MUSCARINIC AGONIST

AGONIST-RECEPTOR INTERACTION

PLASMA  
MEMBRANE



PROPOSED SCHEME OF THE ROLE OF TRIPHOSPHOINOSITIDE IN STIMULUS-RESPONSE  
COUPLING AT  $\alpha$ -ADRENERGIC AND MUSCARINIC RECEPTORS OF IRIS SMOOTH MUSCLE

Observations which supported the involvement of this phosphodiesterase in the "TPI Effect" included the  $\text{Ca}^{++}$ -dependence of the neurotransmitter-stimulated TPI breakdown and PA synthesis (7) and the release of inositol triphosphate upon stimulation by ACh (R.A. Akhtar, unpublished observations). 3) Changes in membrane structure caused by the breakdown of TPI may then lead to increased  $\text{Na}^+$  and  $\text{K}^+$  permeability followed by depolarization of the postsynaptic membrane and, ultimately, contraction of the iris muscle.

## II. Statement of Problem:

As stated previously, studies from Abdel-Latif's laboratory (3) indicated that upon addition of acetylcholine (ACh) or norepinephrine to rabbit iris muscle, that had been prelabeled with  $^{32}\text{P}$ , there was a significant increase in the loss of  $^{32}\text{P}$ -radioactivity from TPI which was accompanied by an increase in the  $^{32}\text{P}$ -labeling of PA and PI. This observed response, termed the "TPI Effect", was shown, through studies with various receptor agonists and blockers, to be associated with activation of cholinergic muscarinic and alpha-adrenergic receptors, respectively. Further investigations have shown that  $\text{Ca}^{++}$  (7) was required for the "TPI Effect" and that surgical sympathetic denervation and *in vivo* electrical stimulation of the sympathetic nerve increased this phenomenon (5). These studies clearly indicated that the observed increase in TPI turnover in response to these neurotransmitters could be involved in the function of cholinergic muscarinic and alpha-adrenergic receptor mechanisms in the iris.

For many tissues, responses resulting from the interaction of agonists with their receptors have been described by the construction of dose-response curves. I have taken this approach in describing the TPI and PA responses to muscarinic receptor activation. Also, for certain physiological responses to receptor activation in smooth muscle, agonist binding to the receptor is the rate-limiting step in the series of reactions leading to the ultimate tissue response (30). Therefore, if TPI and PA turnover are associated with the receptor-mediated pathway leading to iris contraction, one should expect the dissociation constants derived from dose-TPI and dose-PA responses to be similar to those derived from dose-contraction responses.

Studies were undertaken to compare receptor-activated TPI, PA, and contraction responses in the iris muscle. Dose-response curves for each response were constructed, and kinetic constants were determined from these curves.

## MATERIALS AND METHODS

### I. Materials:

#### A. Radioactive and non-radioactive compounds.

[ $^{32}\text{P}$ ] orthophosphate, carrier-free, was obtained from New England Nuclear. Acetylcholine hydrochloride (ACh), carbamylcholine hydrochloride (Carbachol), acetyl- $\beta$ -methacholine, atropine sulfate, eserine sulfate, 2-deoxyglucose, 2,5-diphenyloxazole (PPO), and 1,14-bis (5-phenyloxazol-2-yl) benzene (POPOP) were obtained from Sigma Chemical Company. Silica Gel H was purchased from Brinkman Instruments, Inc., and magnesium acetate, chloroform, methanol, trichloroacetic acid, and toluene were obtained from the Fisher Scientific Company.

#### B. Animals.

Albino rabbits of either sex, weighing approximately 1 kg were purchased from Cook's Rabbitry of Belvedere, South Carolina.

### II. Methods:

#### A. Determination of dose-TPI and dose-PA responses.

##### 1. Preparation of irises.

The rabbits were stunned by a blow to the head and exsanguinated. The eyes were immediately enucleated and placed in a cold Bradford-Tris buffer, pH 7.4 (11).

##### 2. Incubation of irises.

A Bradford medium was used for all incubations (3). This medium contained (in final concentration): 124 mM NaCl, 5 mM KCl, 1.2 mM

$\text{KH}_2\text{PO}_4$ , 1.3 mM  $\text{MgCl}_2$ , 26 mM Tris, 1.6 mM cytidine, 0.75 mM  $\text{CaCl}_2$ , 1.6 mM myoinositol, and 10 mM D-glucose. The pH of the medium was adjusted to 7.4 with 0.1 N HCl. All the incubations were carried out at 37°C.

To radioactively label the phospholipids, the paired irises were transferred to 2 ml of the Bradford medium that contained 25  $\mu\text{Ci}$  of  $^{32}\text{P}$  per ml and incubated for 20 min at 37°C. At the end of incubation, the irises were washed three times with excess nonradioactive Bradford medium that contained 10 mM 2-deoxyglucose. This concentration of 2-deoxyglucose in the washing and subsequent incubation medium was shown in previous work to appreciably decrease the amount of endogenous ATP level in the iris muscle and to prevent further labeling of phospholipids (3). The  $^{32}\text{P}$ -labeled irises were then incubated separately (one of each pair was used as control and the other as experimental) for an additional 15 min in 1 ml of the nonradioactive medium that contained 2-deoxyglucose in the absence and presence of a cholinergic drug. In experiments containing ACh, 0.05 mM eserine (final concentration) was added along with the agonist. When the effects of atropine were studied, the blocker was added to the iris 5 min before the addition of the agonist drug.

### 3. Extraction of phospholipids.

At the end of the 15 min incubation with the various agonist drugs, 1 ml of 10% (w/v) trichloroacetic acid was added to each tube. The irises were then washed twice with 2 ml distilled  $\text{H}_2\text{O}$ , blotted dry, and placed in 2 ml chloroform-methanol-concentrated HCl (300:300:1.5).



Each iris was left for 8 to 12 hours in this solution. Next, the irises were transferred to a similar 2 ml of the chloroform-methanol-HCl solution and were homogenized. The homogenate was centrifuged for 15 min at 3500 rpm and the supernatant poured off and saved. The residue was then extracted with 2 ml of chloroform-methanol-concentrated HCl (400:200:1.5), centrifuged for 15 min at 3500 rpm, and the supernatant poured off. The three extracts were pooled and evaporated under N<sub>2</sub>. The residue from this evaporation was redissolved in 2 ml of chloroform and washed once with 0.5 ml of 0.1 N HCl. The aqueous layer was removed, and the chloroform layer was dried under a N<sub>2</sub> stream. The residue was again dissolved in 2 ml of chloroform and duplicate 0.05 ml aliquots were removed for determination of total counts. The remaining lipid extract was dried under N<sub>2</sub>, the residue dissolved in 0.05 ml chloroform, and spotted on TLC plates.

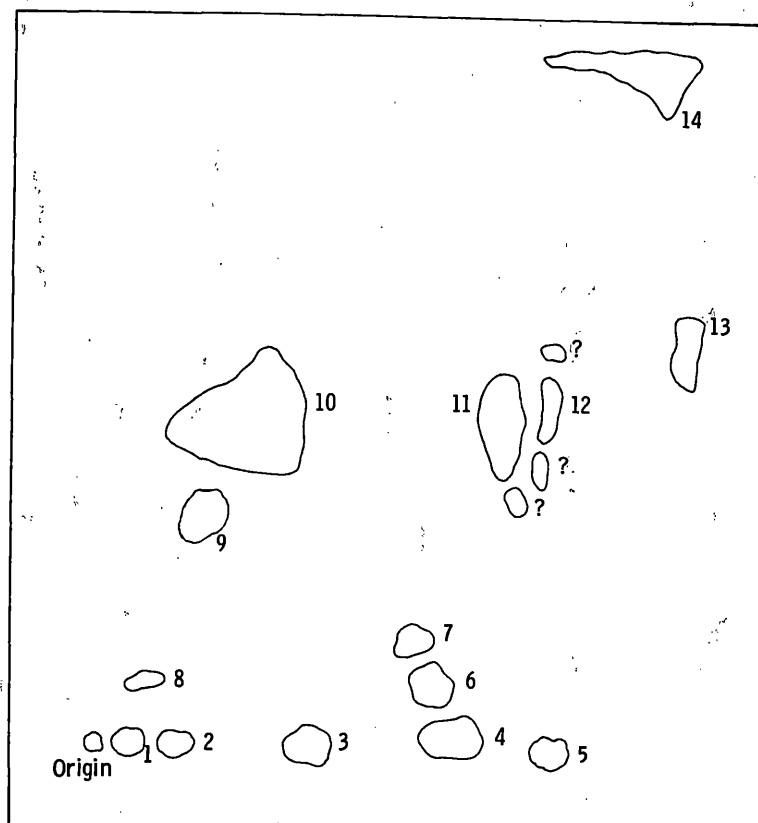
#### 4. Isolation of lipids by thin-layer chromatography (TLC).

The individual phospholipids were isolated by means of two-dimensional TLC (3) (see Fig. 2). A silica gel slurry was prepared by mixing 40 g of silica gel H with 3 g magnesium acetate in 95 ml de-ionized water and spread on 20 x 20 cm glass plates in a layer 0.40 mm thick. After preparation, the plates were allowed to air dry, then were activated for one hour at 110°C. The solvent systems used were the following: first dimension, chloroform-methanol-concentrated ammonium hydroxide (65:25:4); second dimension, n-butanol-acetic acid-water (6:1:1). After removal from the solvent tanks, the plates were allowed to dry

Figure 2. *Separation of iris muscle phospholipids by means of two-dimensional t.l.c.*

Numbers in the figure refer to the following compounds:  
1, triphosphoinositide; 2, diphosphoinositide; 3, diglyceride; 4, phosphatidylserine; 5, phosphatidic acid;  
6, phosphatidylinositol; 7, lysophosphatidylethanolamine;  
8, lysophosphatidylcholine; 9, sphingomyelin; 10, phosphatidylcholine; 11, phosphatidylethanolamine; 12, cardiolipin;  
13, unidentified; 14, cholesterol and neutral lipids.  
(Identified in reference 3.)

Chloroform : Methanol : Ammonia (65 : 25 : 4 by vol)



N-Butanol : Acetic acid : Water (6 : 1 : 1 by vol)

for approximately two hours. The lipids were then visualized with iodine vapor by placing the plates in a glass tank containing iodine crystals. The plates were allowed to remain in the iodine for 30 min. Immediately after removal from the iodine tank, the phospholipids of interest were identified and circled. The iodine was then allowed to evaporate (1-2 hours) before determining radioactivity in the individual phospholipids.

#### 5. Measurement of phospholipid radioactivity.

For counting, the phospholipid spots were scraped from the plates into glass scintillation vials containing 8 ml of the following cocktail: 0.4% 2,5-diphenyloxazole (PPO) and 0.015% 1,4-bis-(5-phenyloxazol-2-yl) benzene (POPOP) in a toluene solution. The vials were then thoroughly mixed and immediately counted on a Beckman Model LS-230 liquid scintillation counter for 5 min each.

#### 6. Construction of dose-TPI and dose-PA response curves.

Dose-response curves to the cholinergic agonists, ACh, acetyl- $\beta$ -methacholine, and carbachol, were constructed for the TPI and PA responses. The stimulatory effect of these drugs on TPI breakdown was measured through the decrease in  $^{32}\text{P}$ -radioactivity in TPI upon addition of various doses of the cholinergic agonist. The maximum TPI response was defined as the dose beyond which further increases in ACh produced no further increase in the loss of radioactivity from TPI. On the right ordinate, response was plotted as percentage of the maximum TPI response; the left ordinate was a measure of the

actual percentage decrease in  $^{32}\text{P}$ -radioactivity from TPI in response to the cholinergic agents. For the PA response, the stimulatory effect of these drugs was measured as the increase in  $^{32}\text{P}$ -radioactivity upon addition of the agonist. Maximum PA response was taken at the dose of ACh beyond which higher concentrations of the neurotransmitter produced no further increases in PA labeling. On the left ordinate, response was plotted as actual percentage increase in  $^{32}\text{P}$ -labeling of PA in response to various concentrations of the drug; on the right ordinate, response was plotted as percentage of the maximum PA response. The maximal TPI and PA responses were plotted as 100% response. For the construction of dose-TPI and dose-PA response studies with atropine, a control curve with ACh only was plotted along with dose-response curves for ACh plus various atropine concentrations.

B. Determination of dose-tension responses.

1. Preparation of irises.

The rabbits were stunned by a blow to the head, exsanguinated, and the eyes enucleated. The iris muscle was isolated from each eye and mounted in an isolated muscle bath containing 50 ml of normal Ringer's solution (pH 7.2) which was continuously oxygenated (97%  $\text{O}_2$ -3%  $\text{CO}_2$ ) and maintained at a constant temperature of  $37^\circ\text{C}$  (12a).

2. Incubation of irises.

The irises were mounted vertically in the muscle chamber by placing ligatures on both ends of the muscle; one end attached to a glass muscle holder and the other to a Grass FT03 force-displacement

transducer. The muscle preparations were equilibrated for 90 min under a resting tension of 200 mg before they were exposed to the cholinergic agents. During equilibration, the tissues were washed with fresh Ringer's solution every 20 min to prevent accumulation of metabolic end products. Isometric contractions were recorded on a Beckman Type R411 Dynograph.

### 3. Determination of the contraction response.

At the end of the initial equilibration period in normal Ringer's solution, isometric contractile responses to increasing concentrations of the agonist were obtained by a cumulative increase in the total concentration of the drug in the bath. Dose-response studies were performed by adding the most dilute concentration of the particular cholinergic agonist to be studied into the bath. Maximum tensions were usually recorded within 1 to 2 minutes after the addition of the agonist. Before the next concentration of agonist is added, the iris was allowed to reach a new steady-state tension. That is, when the tension levels off, the next highest dose is added to the bath at this point. Drug dosages are expressed in terms of the final concentration in the bath.

For dose-contraction studies with ACh plus atropine, control responses in the presence of ACh only were first determined, then the tissues were washed several times with the buffer and allowed to re-equilibrate. Atropine was then added to the bathing medium and the tissues were incubated an additional 60 min before determining the contraction response to ACh.

#### 4. Construction of dose-contraction response curves.

The stimulatory effect of various concentrations of ACh, acetyl- $\beta$ -methacholine, and carbachol on the contraction response of the iris were recorded as the increase in tension observed after addition of the agonist. Maximum response was defined as the maximum tension recorded with ACh (plotted as 100%). All responses were plotted as percentages of this maximum response against the log molar concentration of agonist. For dose-contraction response studies with ACh and atropine, a control curve with ACh only was first determined and plotted along with the curves for ACh plus atropine.

#### C. Calculations and determinations of the kinetic constants from the TPI, PA, and contraction data.

In these experiments, the data were plotted as percent of the maximal biochemical (as well as % of control for TPI and PA) and pharmacological (contraction) responses to the cholinergic agonists. From these curves, the concentration of the agonist resulting in half-maximum response ( $ED_{50}$ ) was determined by a horizontal extrapolation from the 50% maximal level on the right ordinate, across to the dose-response curve, and then by a vertical extrapolation to the abscissa. The dissociation constant for the receptor-agonist complex ( $K_B$ ) was calculated according to the equation  $([A']/[A])^{-1} = [B]/K_B$  where  $[A']/[A]$  (= dose ratio) is the ratio of concentrations of agonist giving an equal response in the presence and in the absence, respectively, of a given concentration  $[B]$  of the antagonist (18). The

analysis requires that the values for the (dose ratio-1) for the agonist plotted against the concentration of antagonist, in their logarithmic forms (Schild plot), fit a straight line with a slope near unity (9). When the  $\log (\text{dose ratio}-1) = 0$  (i.e., when dose ratio = 2), the Schild plot will intercept the abscissa at the point corresponding to the  $pA_2$  value ( $= -\log K_B$ ).

The  $pA_x$  scale was introduced by Arunlakshana and Schild (9) to quantitatively define competitive antagonism:  $pA_x$  is the negative logarithm of the molar concentration of an antagonist that will reduce the effect of a multiple concentration (X) of an agonist to that of a unit concentration. In the simplest interpretation of competitive antagonism, the agonist and antagonist compete for the same binding site; thus, if a plot of  $\log (\text{dose ratio}-1)$  against  $-\log [B]$  is constructed, this should give a straight line with a slope near unity. Calculations for regression analysis and standard error of the mean were carried out on a Monroe 1930 calculator.



## RESULTS

### I. Effect of Incubation Time on the $^{32}\text{P}$ -Radioactivity of TPI and PA After Addition of ACh:

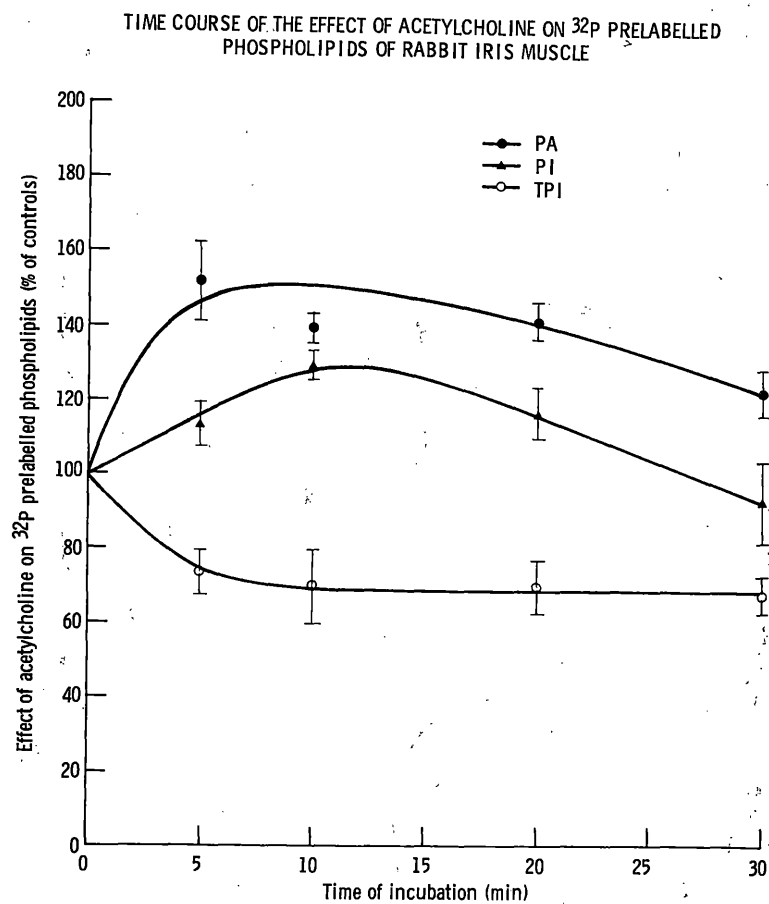
To insure that the phospholipid responses I was measuring for my dose-response studies were the optimum tissue responses, I measured the loss of  $^{32}\text{P}$ -radioactivity from TPI and the increase in  $^{32}\text{P}$ -radioactivity in PA and PI at various time intervals. Figure 3 shows the time-course of changes in TPI, PA and PI radioactivity in response to addition of  $5 \times 10^{-5}$  M ACh. Maximum response was reached after 10 min incubation with ACh at  $37^\circ\text{C}$  and declined thereafter. This showed that the optimum time-interval for measuring the TPI Effect in the iris occurred at 10 min after addition of the neurotransmitter. When irises, which had been prelabeled with  $^{32}\text{P}$ , were incubated for various time-intervals (5 to 30 min) in the absence of ACh, there was a loss of radioactivity from TPI and PA (80 and 60%, respectively) and an increase in that of PI (20%) with time.

### II. Dose-Response Curves (TPI-Breakdown, PA-Labeling, and Contraction Responses) to Various Muscarinic Agonists:

To clarify the relationship between the biochemical (TPI and PA) and pharmacological (contraction) responses, the effects of various concentrations of ACh, carbachol and acetyl- $\beta$ -methacholine on the stimulation of TPI breakdown, PA-labeling and muscle contraction were investigated. The dose-TPI and dose-PA responses for concentrations

Figure 3. *Effect of ACh, at various time intervals, on tissue phospholipids.*

For experimental conditions, see Methods. Prelabelled irises were incubated for various time-intervals in the presence of  $5 \times 10^{-7}$  M ACh + eserine. The effects of acetylcholine are expressed as a percentage of control value  $\pm$  SEM for three different experiments.



of the agonists between  $1 \times 10^{-8}$  M and  $1 \times 10^{-4}$  M are shown in Figures 4 and 5, respectively. Maximal TPI and PA responses were observed with  $1 \times 10^{-4}$  M ACh, which produced a 34% increase in TPI-breakdown (Fig. 4) and a 104% increase in PA-labeling (Fig. 5). Higher concentrations of ACh did not produce further increases in either TPI-breakdown or PA-labeling. Similarly, the dose-tension relationships for ACh, carbachol and acetyl- $\beta$ -methacholine were investigated (Fig. 6). Concentrations of these agonists between  $1 \times 10^{-7}$  M and  $1 \times 10^{-3}$  M caused a concentration dependent contraction on the iris muscle.

The potencies of these agonists were determined based on doses which produced an equal biochemical or pharmacological response. In the present studies, the absolute ED<sub>50</sub> value for each agonist was taken as a measure of its potency. The ED<sub>50</sub> values for the various muscarinic agonists were determined from the dose-response curves in Figures 4, 5, and 6 and are summarized in Table 1. The affinity, obtained with the pharmacological method, for ACh is slightly lower than that obtained with the biochemical method (Table 1). This could be due to the fact that eserine was omitted from the incubation mixture in the former. In contrast, the affinities for acetyl- $\beta$ -methacholine and carbachol obtained with the pharmacological method are higher than those obtained with the biochemical method (Table 1).

III. Dose-Response Curves (TPI-Breakdown, PA-Labeling, and Contraction Responses) to ACh in the Presence and Absence of Atropine and Measurement of Atropine Antagonism:

Figure 4. *Dose-response curves (TPI breakdown) to ACh, methacholine, and carbachol in rabbit iris muscle.*

In these experiments the irises were prelabelled in pairs with  $^{32}\text{P}$ i (25  $\mu\text{Ci}$  per ml in a final volume of 2 ml) for 20 min. at  $37^\circ\text{C}$ . At the end of this incubation, the irises were washed 3 times with non-radioactive incubation medium that contained 10 mM 2-deoxyglucose. The irises were then incubated in the non-radioactive medium plus 2-deoxyglucose in the absence and presence of various concentrations of the agonists for 10 min. at  $37^\circ\text{C}$ . The lipids were extracted, then separated by means of two-dimensional TLC and their radioactive contents determined. The TPI response to the agonist was expressed as either % of the maximal TPI decrease in  $^{32}\text{P}$  labelling or as % decrease in labelling from control. Each point represents the mean of 3-5 separate determinations  $\pm$  SEM.

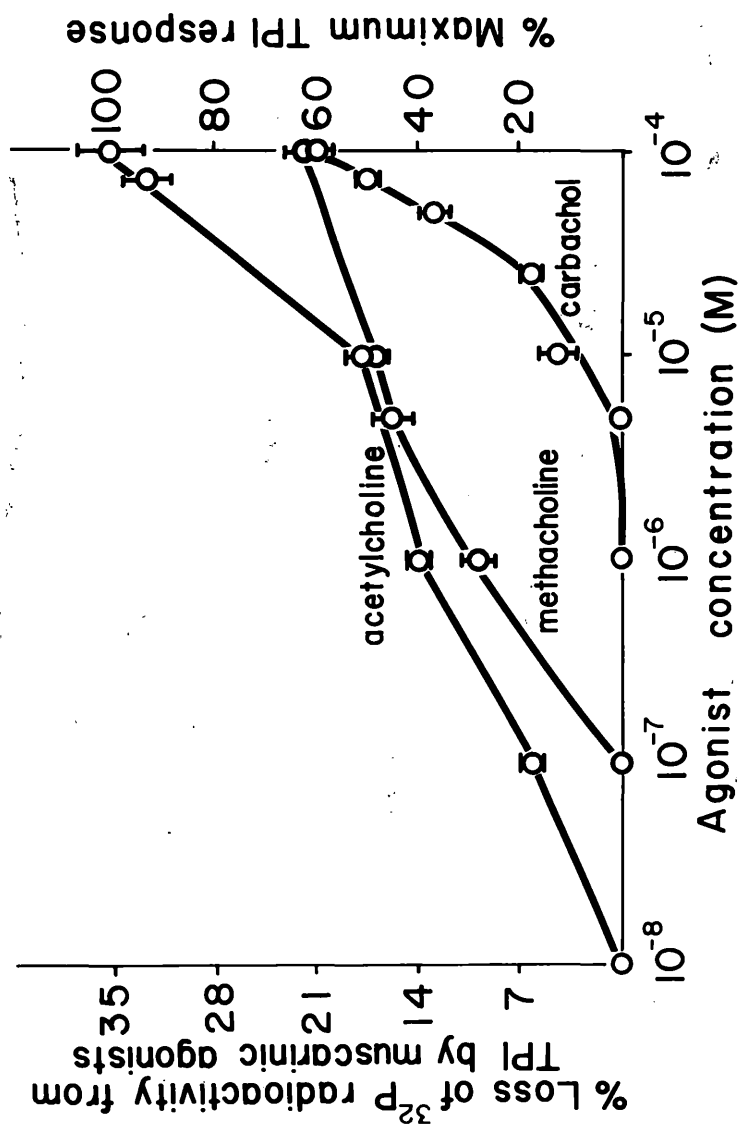


Figure 5. *Dose-response curves (PA-labelling) to ACh, methacholine, and carbachol in rabbit iris muscle.*

Conditions of incubation were as described under Fig. 4. The PA response to the agonist was expressed as either % of the maximal PA increase in  $^{32}\text{P}$  labelling or as % increase in labelling over control. Each point represents the mean of 3-5 individual determinations  $\pm$  SEM.

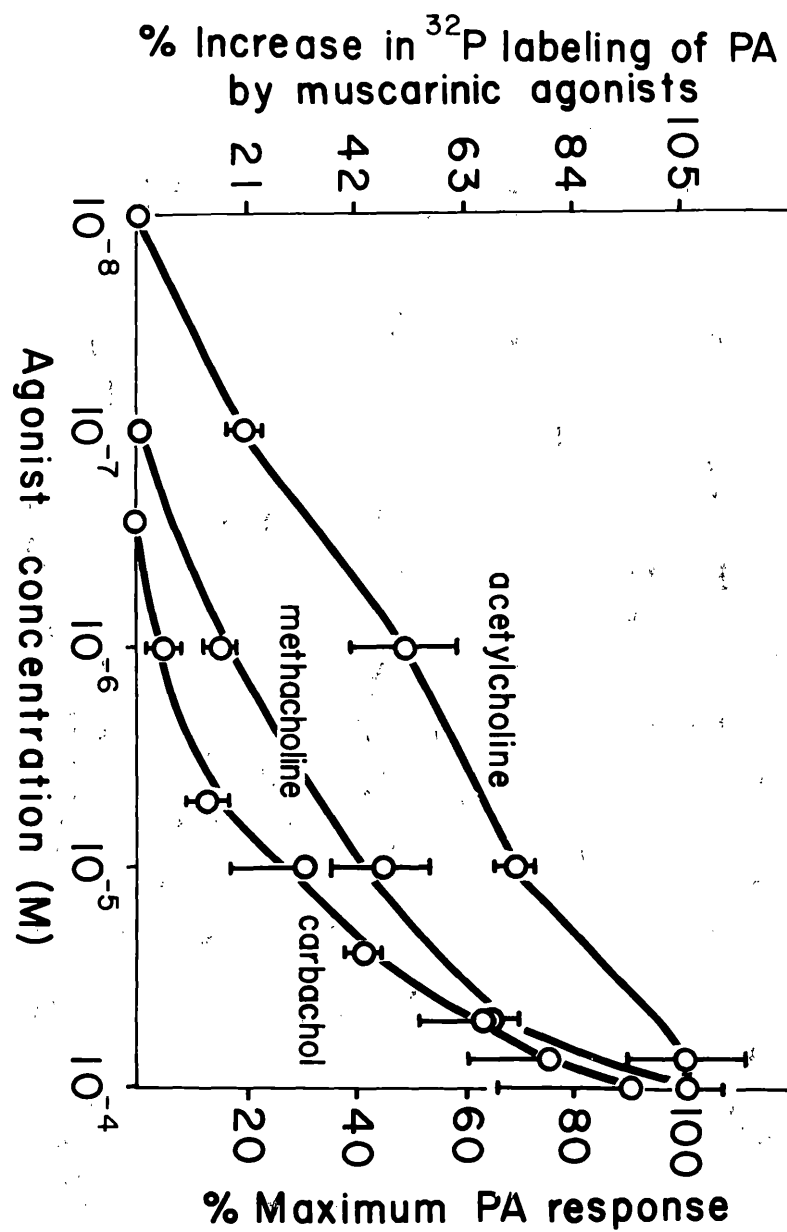




Figure 6. *Dose-response curves (contraction) to ACh, methacholine, and carbachol in rabbit iris muscle.*

Experimental conditions were described in detail in Methods. In brief, isometric contractions to cumulative increases in the concentration of each agonist were recorded. After each recorded contraction, the muscle was allowed to reequilibrate before the next concentration of agonist was added. Response was plotted as a % of the maximum recorded contraction. Each point represents the mean  $\pm$  SEM of 3 individual determinations.

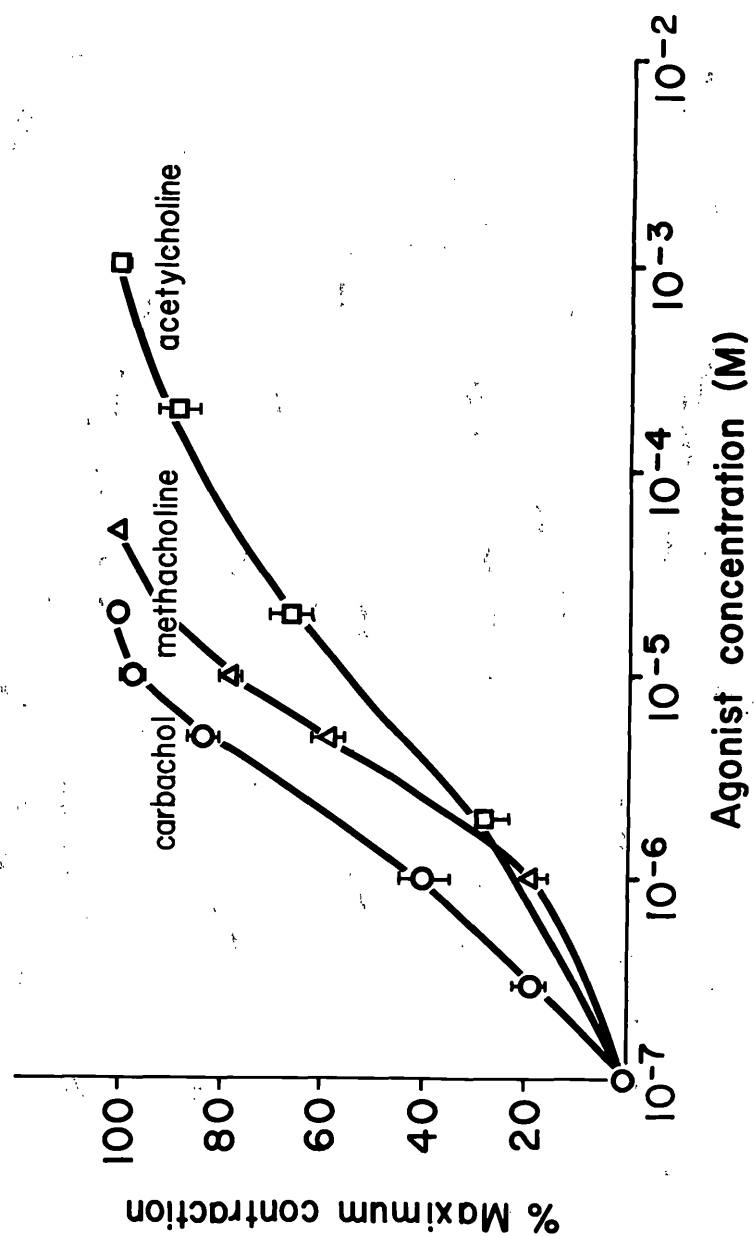


Table 1. *Relative affinities<sup>+</sup> (-log ED<sub>50</sub>) of cholinergic agonists for iris muscle muscarinic receptors obtained from the biochemical and pharmacological methods.*

Agonist	-Log ED <sub>50</sub>		
	Biochemical method <sup>‡</sup>		Pharmacological method
	TPI breakdown	PA-labelling	Muscle contraction
Acetylcholine	5.22	5.92	5.12
Acetyl- $\beta$ -methacholine	4.88	4.82	5.46
Carbachol	4.15	4.48	5.82

<sup>+</sup> These values were calculated from figures 4, 5, and 6, respectively.

<sup>‡</sup> Eserine was included with ACh in these experiments.

To determine the inhibition constant of atropine and to characterize the type of inhibition, the effects of a range of atropine concentrations between  $1 \times 10^{-12}$  M and  $5 \times 10^{-5}$  M were investigated. It was found that at these concentrations, atropine in the absence of any added agonist had no effect on either TPI breakdown or PA-labeling. The sensitivity of the test systems (both biochemical and pharmacological) was reduced by addition of increasing concentrations of atropine to the incubation medium (Figures 7, 8, and 9). With concentrations of atropine of  $1 \times 10^{-8}$  M,  $1 \times 10^{-9}$  M, and  $1 \times 10^{-10}$  M, the ACh-stimulated breakdown of TPI and labeling of PA were inhibited (Figures 7 and 8). It was found that higher concentrations of ACh could partially overcome this blocking activity of atropine. As expected, increasing concentrations of atropine progressively shifted the dose-TPI and dose-PA response curves to the right in a near parallel fashion (Figures 7 and 8). Similarly, in the presence of  $1 \times 10^{-8}$  M and  $1 \times 10^{-9}$  M atropine, the dose-tension curve to ACh was shifted to the right in a near parallel fashion (Fig. 9).

In order to ascertain that the inhibitory effect of atropine (Figures 7, 8, and 9) involved a competitive reversible inhibition according to receptor theory and to allow for calculation of the dissociation constant for the receptor-antagonist complex ( $K_B$ ), the log dose ratio-1 was plotted as a function of the negative logarithm of the atropine concentration (Figures 10, 11, and 12) according to

Figure 7. *Dose-response curves (TPI breakdown) to ACh in the absence and presence of atropine in the rabbit iris muscle.*

Experimental conditions are the same as described in Fig. 4. In those irises where the effects of atropine was studied, the blocker was added 5 min. before addition of ACh. The TPI response was expressed either as % of the maximal TPI decrease in  $^{32}\text{P}$  labelling or as % decrease of  $^{32}\text{P}$  labelling in TPI from control. Each point represents the mean of 3-5 separate determinations  $\pm$  SEM.

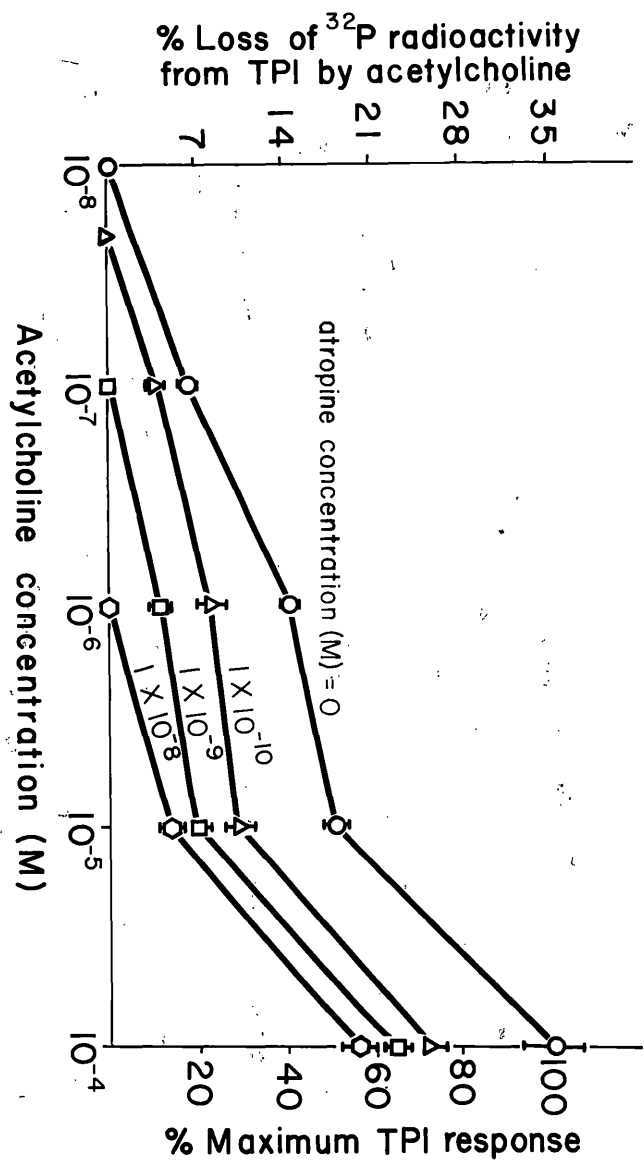


Figure 8. *Dose-response curves (PA-labelling) to ACh in the absence and presence of atropine in the rabbit iris muscle.*

Experimental conditions are described under Fig. 4. In those samples containing atropine, the blocker was added 5 min. before addition of ACh. The PA response was expressed either as % of the maximal increase in  $^{32}\text{P}$ -labelling in PA or as % increase in  $^{32}\text{P}$ -labelling of PA over the control. Each point represents the mean of 3-5 separate determinations  $\pm$  SEM.

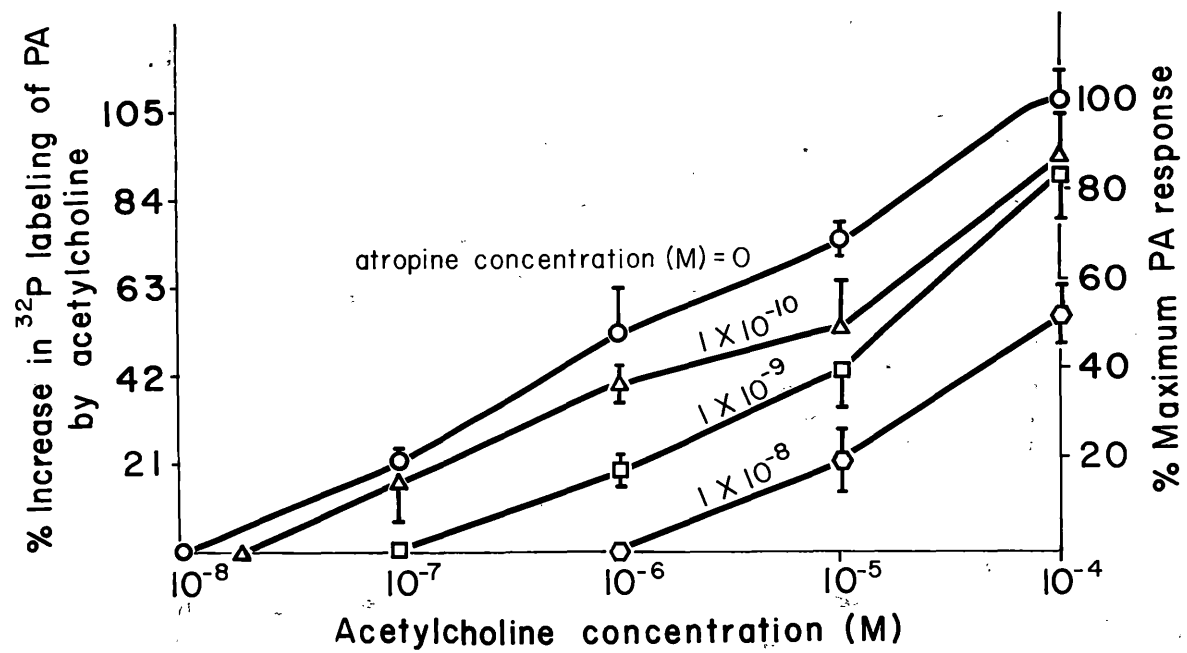
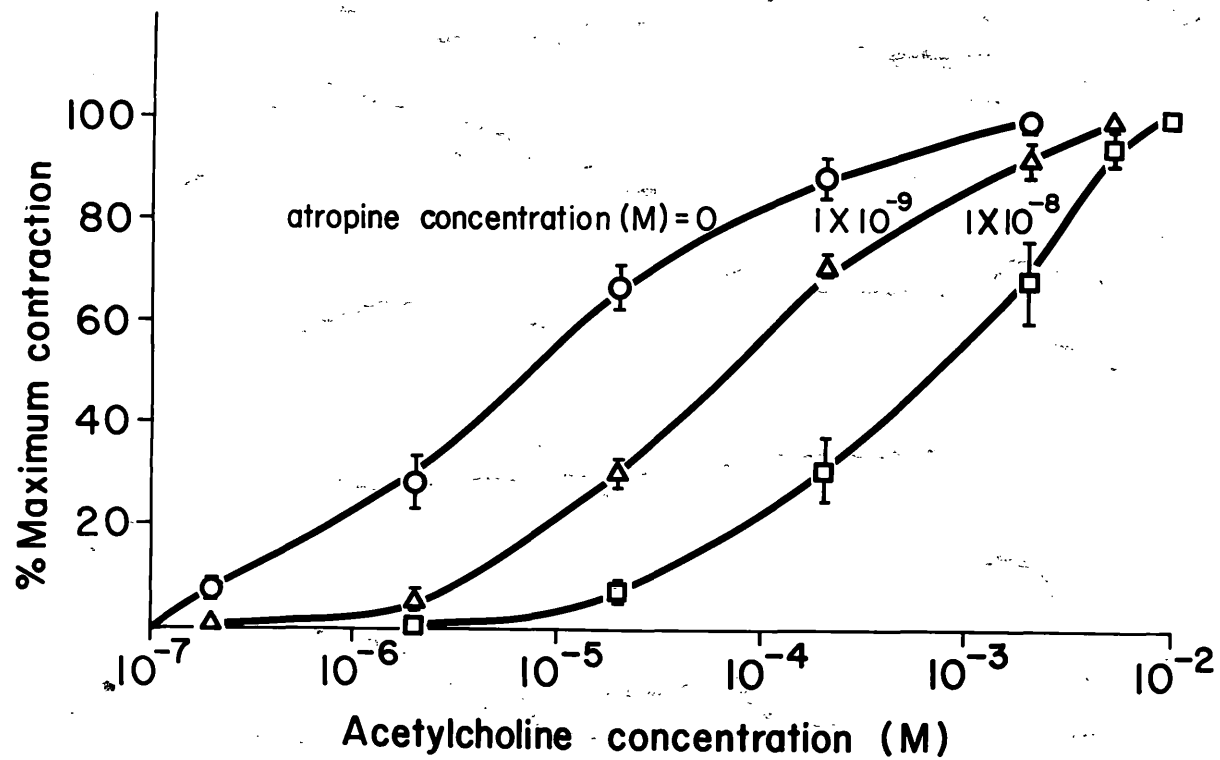




Figure 9. *Dose-response curves (contraction) to ACh in the absence and presence of atropine in rabbit iris muscle.*

See Methods for experimental conditions. Control responses to ACh only were determined first. The muscles were then washed, allowed to re-equilibrate, and atropine was added. The tissues were incubated an additional 60 min. in the presence of atropine before the addition of ACh. Isometric contractions to ACh stimulation were recorded, and response was plotted as % of the maximum recorded contraction to ACh. Each point represents the mean  $\pm$  SEM of 3 individual determinations.



Arunlakshana and Schild (9). The points where these plots intercept the abscissa (at  $\log [\text{dose ratio} - 1] = 0$ ) is defined as the  $pA_2$  (Figures 10, 11, and 12). The slopes obtained from the Schild plots in Figures 10, 11, and 12 were found to be -0.80, -0.85, and -1.03, respectively. These values are sufficiently near unity to be consistent with the antagonist acting in a competitive manner with ACh for the receptor (21, 11b). The calculated  $K_B$  values (see 'Methods') and the corresponding  $pA_2$  values are summarized in Table 2.

Figure 10. *Arunlakshana-Schild plot based on the dose-response curves for ACh and atropine with the TPI response (see Fig. 7).*

The  $pA_2$  value is the negative logarithm of the atropine concentrations which requires twice as high a concentration of ACh to stimulate a given response. The line of best fit for the point was determined by linear regression analysis.

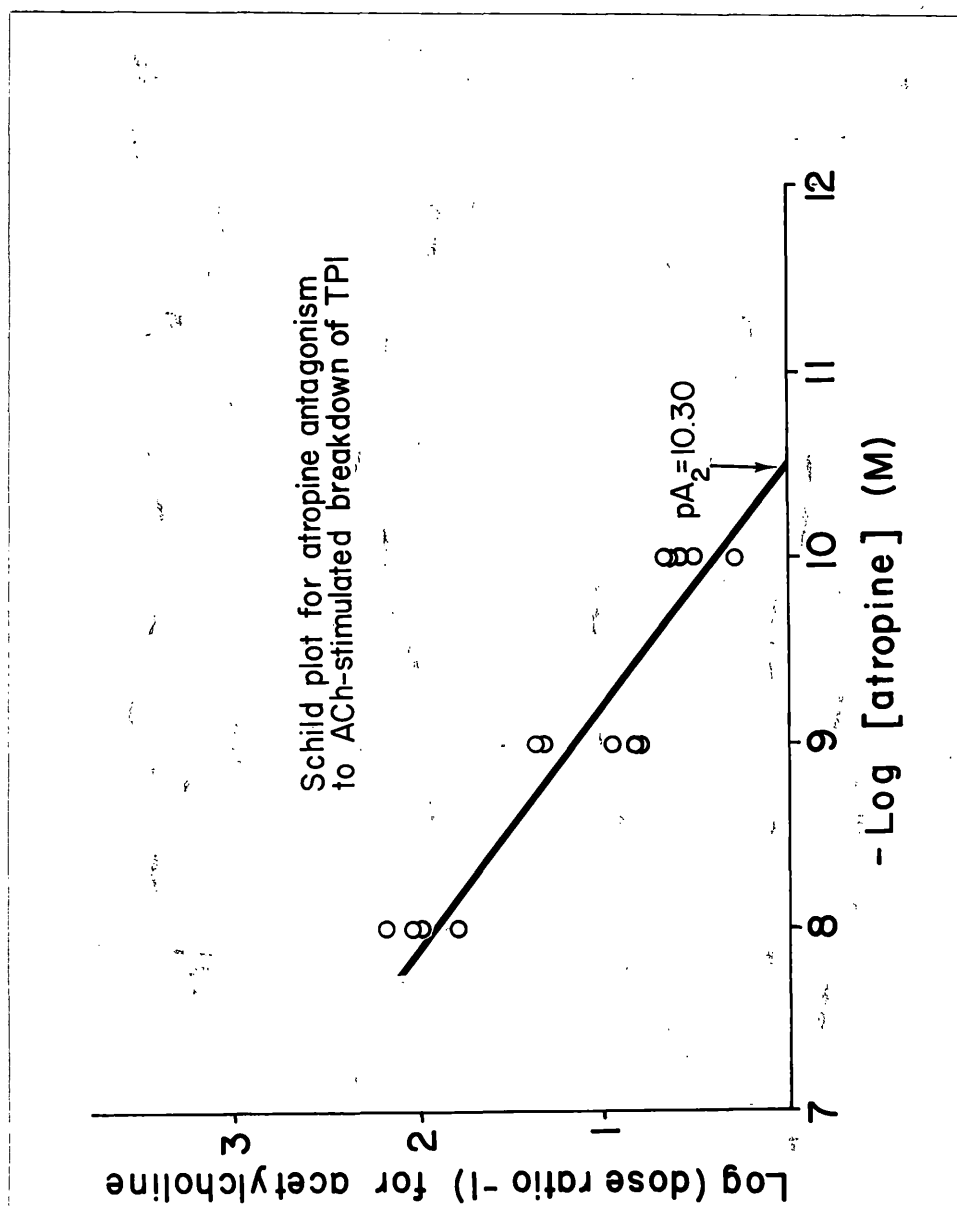


Figure 11. *Arunlakshana-Schild plot based on the dose-response curves for ACh and atropine with the PA response (see Fig. 8).*

For definition of  $pA_2$ , see Fig. 7. The line of best fit through the points was determined by linear regression analysis.

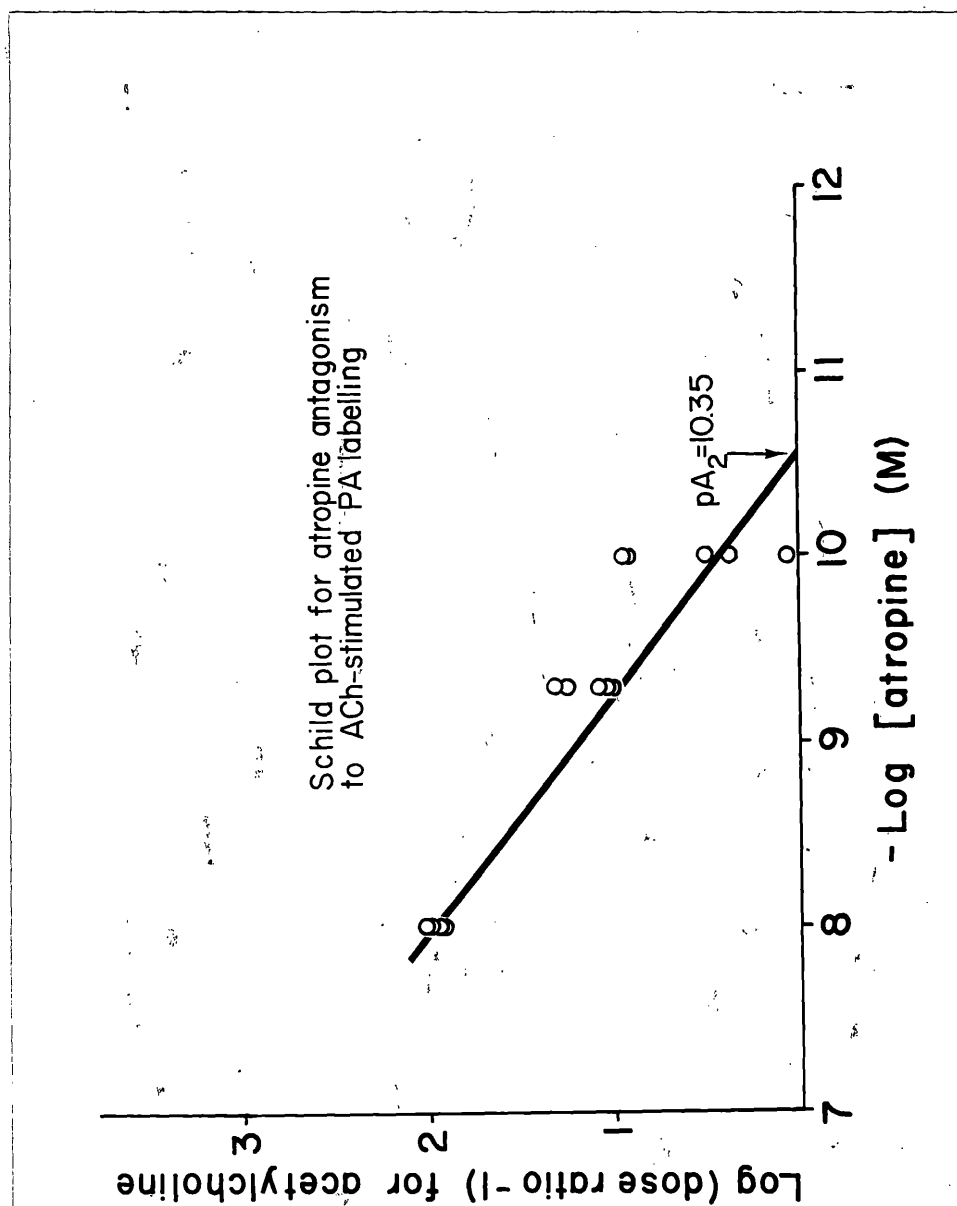


Figure 12. *Arunlakshana-Schild plot for the dose-response curves to ACh and atropine for the contraction response (see Fig. 9).*

For definition of  $pA_2$ , see Fig. 7.



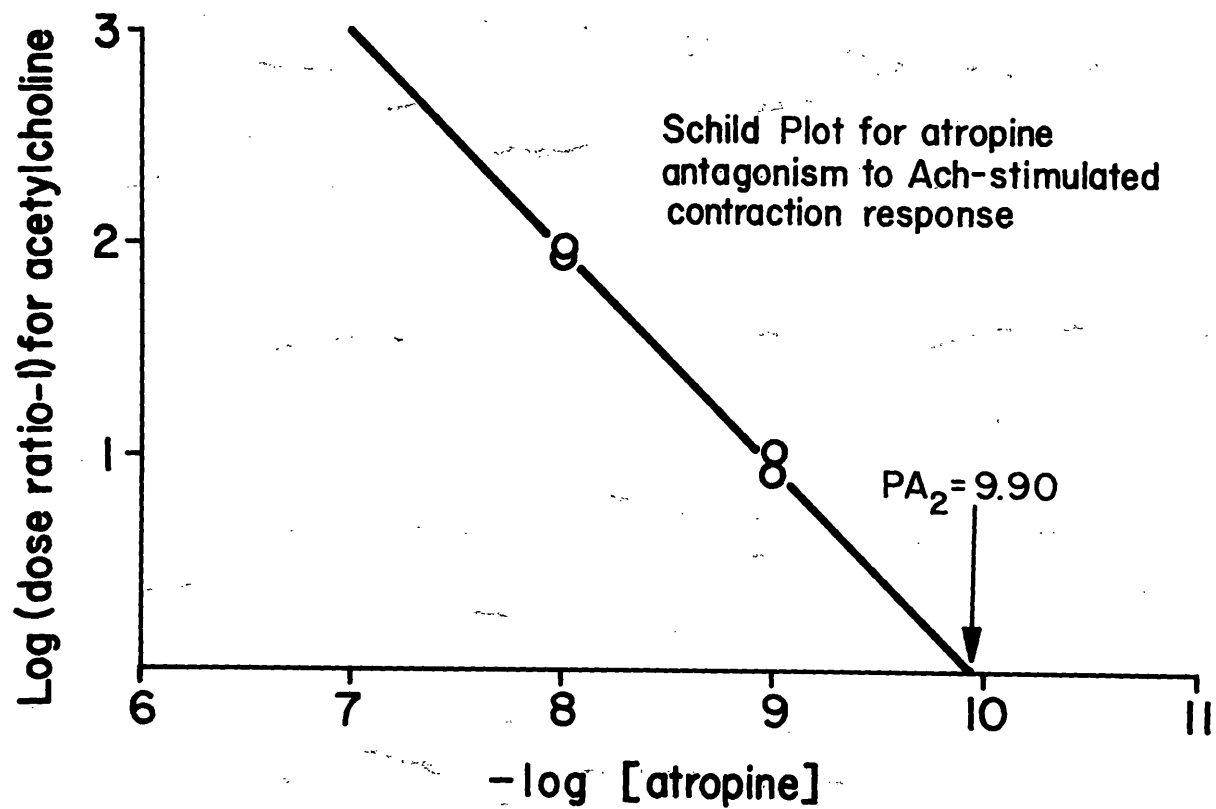


Table 2. *Dissociation constants for the atropine-muscarinic receptor complex obtained from the biochemical\* and pharmacological\*\* methods.*

Method of Determination	$pA_2$	$-(\text{Log}) K_B$
TPI Response	10.30	9.76 (15) <sup>†</sup>
PA Response	10.35	8.70 (22)
Contraction Response	9.90	9.94 (6)

\* Calculated from figures 7, 8, 10, and 11.

\*\* Calculated from figures 9 and 12.

† Total number of individual determinations.

## DISCUSSION

A wide variety of tissues undergo a change of functional state after exposure to neurotransmitters (28,29). To produce this change of state (or response), the neurotransmitter must first interact with its receptor. In the rabbit iris muscle, it was shown that upon addition of ACh there are changes in the radioactive labeling of certain acidic phospholipids and in muscle tension (1-5). It was desirable to determine whether or not these two different responses could be linked through a common receptor-activated pathway. In the present study, pharmacological procedures were applied in which selected cholinergic muscarinic agonists and atropine were used to reveal similarities in the characteristics of these responses. The basic assumption was made that similarities, or differences, in the characteristics of different responses reflect similarities, or differences, in the receptors mediating these responses (21).

The principle procedures used in this study were of two kinds. In the first procedure, the potencies of a series of cholinergic agonists for eliciting biochemical and pharmacological responses in the iris were determined and compared. In the second procedure, the ability of cholinergic drugs to antagonize or block these responses to ACh were determined. The finding of similar kinetic constants for several agonists for stimulating the TPI, PA, and contraction responses were significant indications that the TPI, PA, and contraction responses

in the rabbit iris were all linked through a common locus of control--the muscarinic receptor. Furthermore, an increasing number of studies have shown reasonably good agreement between kinetic constants derived from the pharmacological testing of tissue responses, as shown for various smooth muscle preparations (Table 3).

In the present study, the construction of dose-response curves for the TPI, PA, and contraction responses to cholinergic agonist stimulation enabled us to make quantitative comparisons between these responses. Cholinergic agonist-induced TPI-breakdown and PA-labeling, but not PI-labeling, were found to respond in a dose-dependent manner (Figures 4 and 5), which correlated well with the dose-contraction curves (Fig. 6). For ACh, the kinetic constants ( $ED_{50}$ ) for the rabbit iris contraction, TPI, and PA responses were comparable. Also, our values correlated well with those found for guinea-pig ileum by the radioligand binding procedures, all being of the order of  $1-8 \times 10^{-6}$  M. Similarly, the kinetic constants, for the TPI, PA, and contraction responses in rabbit iris, obtained in the presence of carbachol and acetyl- $\beta$ -methacholine by the above procedures showed good agreement, there being no more than a few-fold difference in either case (Table 3).

Atropine has previously been shown to be a competitive antagonist of ACh at muscarinic receptors (9), and evidence was therefore sought to determine whether atropine could competitively inhibit ACh-stimulated responses in the rabbit iris. For measurement of antagonism, in the present study the effects of atropine on ACh stimulation of the TPI,

Table 3. Comparison of Kinetic Constants Derived from Binding, Contraction, and Biochemical Responses in Smooth Muscle.

Ligand	Method	Preparation	Kinetic Constants (M)				Reference
			Binding	ED <sub>50</sub>	K <sub>B</sub>	pA <sub>2</sub>	
Acetylcholine	ID <sub>50</sub> against [3H]-QNB binding	guinea pig ileum	2-4 x 10 <sup>-6</sup>				41
	Contraction	bovine iris sphincter		3.8 x 10 <sup>-4</sup>			40
	Contraction	guinea pig ileum		5.8 x 10 <sup>-8</sup>			22
	Contraction	brain vessels		1.76x 10 <sup>-6</sup>			16
	Contraction	rabbit iris		7.6 x 10 <sup>-6</sup>			*
	TPI	rabbit iris		1.2 x 10 <sup>-6</sup>			*
	PA	rabbit iris		6.02x 10 <sup>-6</sup>			*
Carbachol	ID <sub>50</sub> against binding of [3H] QNB	guinea pig ileum	2-3 x 10 <sup>-5</sup>				41
	Contraction	bovine iris sphincter		9.3 x 10 <sup>-8</sup>			40
	Contraction	guinea pig ileum		0.5-3 x 10 <sup>-7</sup>			22
	Contraction	guinea pig ileum		1.1 x 10 <sup>-7</sup>			36
	PI Breakdown	guinea pig ileum		1 x 10 <sup>-5</sup>			29
	Contraction	rabbit iris		1.5 x 10 <sup>-6</sup>			*
	TPI	rabbit iris		7 x 10 <sup>-5</sup>			*
	PA	rabbit iris		3.3 x 10 <sup>-5</sup>			*
Acetyl-β-Methacholine	ID <sub>50</sub> against binding of [3H] QNB	guinea pig ileum	3-5 x 10 <sup>-6</sup>				41
	Contraction	bovine iris sphincter		5.2 x 10 <sup>-6</sup>			40
	Contraction	guinea pig ileum		3.3 x 10 <sup>-8</sup>			36
	Contraction	rabbit iris		3.4 x 10 <sup>-6</sup>			*
	TPI	rabbit iris		1.3 x 10 <sup>-5</sup>			*
	PA	rabbit iris		1.5 x 10 <sup>-5</sup>			*
Acetylcholine-Atropine Antagonism	Contraction	guinea pig ileum			1 x 10 <sup>-9</sup>	8.6	9
	Contraction	brain vessels			1 x 10 <sup>-10</sup>	10.1	16
	Contraction	rabbit iris			1.14 x 10 <sup>-10</sup>	9.9	**
	TPI	rabbit iris			1.7 x 10 <sup>-10</sup>	10.3	**
	PA	rabbit iris			2 x 10 <sup>-9</sup>	10.35	**

\* Table 1 in the present study

\*\* Table 2 in the present study

PA, and contraction responses were investigated. Atropine at increasing concentrations from  $1 \times 10^{-10}$  M to  $1 \times 10^{-8}$  M progressively shifted the dose-TPI, -PA, and -contraction response curves to ACh to the right. In contrast to the contraction response where the atropine inhibition was surmounted by concentrations of ACh up to  $1 \times 10^{-3}$  M to  $1 \times 10^{-2}$  M, atropine inhibition of ACh-stimulated TPI breakdown and PA labeling was only partially reversed by  $10^{-4}$  M ACh (Figures 7 and 8). This could have been due to the fact that ACh at high concentrations ( $1 \times 10^{-3}$  M to  $1 \times 10^{-2}$  M) exerts an inhibitory effect on TPI breakdown and PA-labeling (see Figures 7 and 8). Furthermore, in the case of many reversible, competitive antagonists, a steady-state level of blockade is not achieved unless one has allowed the tissue to be in contact with the antagonists for long periods (up to 60 min for blockade of the contraction response with atropine). This is impractical in our biochemical procedure since such long incubation periods will bring about a greater than 90% loss in  $^{32}\text{P}$ -radioactivity from TPI. Since the  $\text{pA}_2$  and  $K_B$  values calculated in my studies may be obtained before a final steady-state level of blockade by atropine has been reached, these constants are a measure of the "apparent" dissociation constant for the atropine antagonism of the ACh-stimulated responses (20).

When these inhibitory effects of atropine were tested for competitive antagonism in the form of a Schild plot (9) for the TPI, PA, and contraction responses, a straight line with a slope near unity

was obtained for each response. The slopes for the TPI- and PA-Schild plots (-.80 and -.85, respectively) were lower than the slope obtained for the contraction-Schild plot (-1.03). The inability to reach a true pharmacological maximum in the ACh-stimulated TPI and PA responses could be responsible for these lower values in slope. These Schild plots provided evidence that atropine produced a parallel shift in the dose-TPI, -PA, and -contraction response curves by competing with ACh for the muscarinic receptor. Thus, the finding of similar  $K_B$  values, calculated from the dose ratios produced by the shift in the ACh dose-response curves, along with similar  $pA_2$  values from the Schild plots (Table 3), are in accord with the hypothesis that in this tissue, TPI breakdown may be involved in the series of events associated with neurotransmitter-receptor interaction and the observed muscle contraction.

Dose-response relationships for the muscarinic receptor-activated TPI and PA responses in the rabbit iris have not been previously described. Indeed, thus far only very few attempts have been made to apply pharmacological procedures to detect those biochemical responses which might be intrinsic to receptor mechanisms. For example, in studies on muscarinic receptor systems in mouse pancreas and guinea-pig ileum, Michell *et al.* (29) constructed dose-response curves to ACh- and carbachol-stimulated increases in phosphatidylinositol (PI) metabolism. They showed a similarity between the dose-response curves for PI metabolism and receptor occupation, from which they predicted a close relationship between PI metabolism and muscarinic receptor activation.

Hanley and Iverson (23) in their studies with rat corpus striatum, compared muscarinic receptor binding studies of various cholinergic agonists with their ability to elicit changes in cGMP. They found similar values for the ED<sub>50</sub> of cholinergic agonists in stimulating cGMP response and for the ID<sub>50</sub> of <sup>3</sup>H-quinuclidinyl benzilate (QNB), thus indicating a relationship between inhibition of the cGMP response and receptor occupancy. <sup>3</sup>H-QNB is a potent antagonist used in studies for specific muscarinic cholinergic binding (41,42).

For the muscarinic receptor in rabbit iris muscle (1), complete radioligand binding studies have not yet been performed. Preliminary studies with unlabeled QNB (a gift from Hoffman-LaRoche) have shown that increasing concentrations progressively inhibit ACh-stimulated TPI-breakdown and PA-labeling. Concentrations of QNB from  $1 \times 10^{-12}$  M to  $1 \times 10^{-5}$  M inhibited the stimulation of the TPI response from 22 to 100% and the PA response from 30 to 100%. Further studies in this laboratory are being conducted by Mr. William Taft with <sup>3</sup>H-QNB in the presence of cholinergic agonists and antagonists. Through his studies, muscarinic receptor binding constants can be derived and compared with the constants derived from my pharmacological studies on the TPI, PA, and contraction responses. Similarities between these constants could provide further evidence linking the TPI Effect to the mechanism of the activated muscarinic receptor.



## SUMMARY

1. Triphosphoinositide breakdown, phosphatidic acid labelling, and muscle contraction were shown to behave in a dose-responsive manner to acetylcholine, acetyl- $\beta$ -methacholine, and carbachol. The concentrations of these agonists employed were from  $1 \times 10^{-8}$  M to  $1 \times 10^{-3}$  M. Maximal TPI and PA responses were observed with  $1 \times 10^{-4}$  M acetylcholine. Maximal TPI response was a 34% increase in breakdown, and maximal PA response was an increase in labelling of 104% over the control. The  $ED_{50}$  for the various cholinergic agents were determined from the dose-response curves. Good correlation between  $ED_{50}$  values determined by the biochemical and pharmacological methods, being of the order 1 to  $8 \times 10^{-6}$  M, were observed.
2. Atropine alone was shown to exert no effect on phospholipid labelling. The stimulatory effects of acetylcholine on TPI breakdown, PA labelling, and muscle contraction were inhibited by atropine. At concentrations between  $1 \times 10^{-10}$  M and  $1 \times 10^{-8}$  M, atropine progressively shifted the dose-TPI, dose-PA, and dose-contraction curves to the right.
3. When the inhibitory effects of atropine on ACh-stimulated TPI breakdown, PA labelling, and muscle contraction were tested for competitive, reversible antagonism in the form of an Arunlakshana-Schild plot, results indicated that inhibition was due to reversible

competition between acetylcholine and atropine for the muscarinic receptors. Similar values for the negative log of the atropine-muscarinic receptor dissociation constant ( $pA_2$ ) were calculated from the X-intercept of the Schild plots for atropine for the TPI response, 10.30, for the PA response, 10.35, and for the contraction response, 9.90.

4. Estimations of the atropine-receptor dissociation constant,  $K_B$ , were calculated from the dose-ratios measured on dose-response curves with acetylcholine plus and minus atropine. The values calculated were 9.76 ( $1.7 \times 10^{-10}$  M) for the TPI responses, 8.70 ( $2 \times 10^{-9}$  M) for the PA response, and 9.90 ( $1.14 \times 10^{-10}$  M) for the contraction response.
5. The findings of similar  $K_B$  values for the atropine muscarinic receptor, along with similar  $pA_2$  values from the Schild plots, with the TPI, PA, and contraction responses in the iris are in accord with the hypothesis that in this tissue TPI breakdown is involved in the chain of events leading from cholinergic muscarinic stimulation to muscle response.

## References

1. Abdel-Latif, A.A. 1976. Effects of neurotransmitters and neuropharmacological agents on phospholipid metabolism in the rabbit iris muscle. *In* Function and Metabolism of Phospholipids in the Central and Peripheral Nervous System; G. Porcellati, L. Amaducci, and C. Galli, eds. Plenum Press, New York, p. 227-256.
2. Abdel-Latif, A.A., M.P. Owen, and J.L. Matheny. 1976. Adrenergic and cholinergic stimulation of  $^{32}\text{P}$ -labelling of phospholipids in rabbit iris muscle. *Biochem. Pharm.* 25: 461-469.
3. Abdel-Latif, A.A., R.A. Akhtar, and J.N. Hawthorne. 1977. Acetylcholine increases the breakdown of triphosphoinositide of rabbit iris muscle prelabelled with [ $^{32}\text{P}$ ] phosphate. *Biochem. J.* 162: 61-73.
4. Abdel-Latif, A.A., R.A. Akhtar, and J.P. Smith. 1978. Studies on the role of triphosphoinositide in cholinergic mescarinic and  $\alpha$ -adrenergic receptors function of iris smooth muscle. *In* Cyclitols and Phosphoinositides; F. Eisenberg and W.W. Well, eds. Acad. Press, New York, p. 121-143.
5. Abdel-Latif, A.A., K. Green, J.P. Smith, J.C. McPherson, and J.L. Matheny. 1978. Norepinephrine-stimulated breakdown of triphosphoinositide of rabbit iris smooth muscle: Effects of surgical sympathetic denervation and *in vivo* electrical stimulation of the sympathetic nerve of the eye. *J. Neurochem.* 30: 517-525.
6. Akhtar, R.A. and A.A. Abdel-Latif. 1978. Studies on the properties of triphosphoinositide phosphomonoesterase and phosphodiesterase of rabbit iris smooth muscle. *Biochim. Biophys. Acta* 527: 159-170.
7. Akhtar, R.A. and A.A. Abdel-Latif. 1978. Calcium ion requirements for acetylcholine-stimulated breakdown of triphosphoinositide in rabbit iris smooth muscle. *J. Pharm. Exp. Ther.* 204: 655-668.
8. Alhquist, R. 1948. A study of the adrenotropic receptors. *Amer. J. Physiol.* 153: 586-600.
9. Arunlakshana, O. and H.O. Schild. 1959. Some quantitative uses of drug antagonists. *Brit. J. Pharm.* 14: 48-58.
10. Birnberger, A.C., K.L. Birnberger, S.G. Eliasson, and P.C. Simpson. 1971. Effect of cyanide and electrical stimulation on phosphoinositide metabolism in lobster nerves. *J. Neurochem.* 18: 1291-1298.

- 11a. Bradford, H.F. 1969. Respiration *in vitro* of synaptosomes from mammalian cerebral cortex. J. Neurochem. 16: 675-684.
- 11b. Bristow, M.R. and R.D. Green. 1977. Effect of diazoxide, verapamil, and Compound D600 on isoproterenol and calcium-mediated dose-response relationships in isolated rabbit atrium. Eur. J. Pharmacol. 45: 267-279.
- 12a. Carrier, G.A. and R.P. Ahlquist. 1976. The influence of extracellular calcium on muscarinic receptors in vascular smooth muscle. Arch. Int. Pharmacodyn. 223: 223-230.
- 12b. Chang, H.W. and E. Neumann. 1976. Dynamic properties of isolated acetylcholine receptor proteins: Release of calcium ions caused by acetylcholine binding. Proc. Natl. Acad. Sci. USA 73: 3364-3368.
13. Chang, K.J. and D.J. Triggle. 1973. Quantitative aspects of drug-receptor interactions. I.  $\text{Ca}^{++}$  and cholinergic receptor activation in smooth muscle: A basic model for drug-receptor interactions. J. Theor. Biol. 40: 125-154.
14. Cho, T.M., J.S. Cho, and H.H. Loh. 1978. Alteration of the physico-biochemical properties of triphosphoinositide by nicotinic ligands. Proc. Natl. Acad. Sci. USA 75: 784-788.
15. Durell, J., J.T. Garland, and R.O. Friedel. 1969. Acetylcholine action: Biochemical aspects. Science 165: 862-866.
16. Edvinsson, L., B. Falck, and C. Owman. 1977. Possibilities for a cholinergic action on smooth musculature and on sympathetic axons in brain vessels mediated by muscarinic and nicotinic receptors. J. Pharm. Exp. Ther. 200: 117-126.
17. Furchgott, R.F. 1959. The receptors for epinephrine and norepinephrine (adrenergic receptors). Pharmacol. Rev. 11: 429-441.
18. Furchgott, R.F. 1964. Receptor mechanisms. Ann. Rev. Pharm. 4: 21-50.
19. Furchgott, R.F. 1966. The use of beta-haloalkylamines in the differentiation of receptors and the determination of dissociation constants of receptor-agonist complexes. Adv. Drug Res. 3: 21-55.
20. Furchgott, R.F. 1970. Pharmacological characteristics of adrenergic receptors. Fed. Proc. 29: 1352-1361.

21. Furchgott, R.F. 1972. The classification of adrenoreceptors. An evaluation from the standpoint of receptor theory. In Handbook of Experimental Pharmacology: Catecholamines; H. Blaschko and E. Muscholl, eds. Springer-Verlag, New York, p. 283-335.
22. Furchgott, R.F. 1978. Pharmacological characterization of receptors: Its relation to radioligand-binding studies. Fed. Proc. 37: 115-120.
23. Hanley, M.R. and L.L. Iverson. 1978. Muscarinic cholinergic receptors in rat corpus striatum and regulation of guanosine cyclic 3',5'-monophosphate. Mol. Pharmacol. 14: 246-255.
24. Hendrickson, H.S. and J.L. Reinertsen. 1969. Comparison of metal-binding properties of trans-1,2-cyclohexanedioldiphosphate and deacylated phosphoinositides. Biochem. 8: 4855-4858.
25. Hendrickson, H.S. and J.L. Reinertsen. 1971. Phosphoinositide inter-conversion: A model for control of  $\text{Na}^+$  and  $\text{K}^+$  permeability in the nerve axon membrane. Biochem. Biophys. Res. Commun. 44: 1258-1264.
26. Hokin, L.E. 1965. Autoradiographic localization of the ACh-stimulated synthesis of PI in the superior cervical ganglion. Proc. Natl. Acad. Sci. USA 53: 1369-1376.
27. Kai, M. and J.N. Hawthorne. 1969. Physiological significance of polyphosphoinositides in the brain. Ann. N.Y. Acad. Sci. 165: 761-773.
28. Michell, R.H. 1975. Inositol phospholipids and cell surface receptor function. Biochim. Biophys. Acta 415: 81-147.
29. Michell, R.H., S.S. Jafferji, and L.M. Jones. 1976. Receptor occupancy dose-response curve suggests that phosphatidylinositol breakdown may be intrinsic to the mechanism of the muscarinic cholinergic receptor. FEBS Letters 69: 1-5.
30. Miller, J. 1977. A study of the kinetics of the muscarinic effect on phosphatidylinositol and phosphatidic acid metabolism in rat brain synaptosomes. Biochem. J. 168: 549-555.
31. Palmer, F.B. and R.J. Rossiter. 1965. A simple procedure for the study of inositol phosphatides in cat brain slices. Can. J. Biochem. 43: 671-683.
32. Quilliam, J.P. 1949. A quantitative method for the study of the reactions of the isolated cat's iris. J. Physiol. 110: 237-247.

33. Schacht, J. and B.W. Agranoff. 1972. Effects of acetylcholine on labelling of phosphatidate and phosphoinositides by [ $^{32}\text{P}$ ] orthophosphate in nerve ending fractions of guinea pig cortex. *J. Biol. Chem.* 247: 771-777.
34. Ticku, M.K. and D.J. Triggle. 1976. Calcium and the muscarinic receptor. *Gen. Pharm.* 7: 133-140.
35. Torda, C. 1974. Model of molecular mechanism able to generate a depolarization-hyperpolarization cycle. *Int. Rev. Neurobiol.* 16: 1-66.
36. Ward, D. and J.M. Young. 1977. Ligand binding to muscarinic receptors in intact longitudinal muscle strips from guinea-pig intestine. *Brit. J. Pharm.* 61: 189-197.
37. White, G.L. and M.G. Larrabee. 1973. Phosphoinositides and other phospholipids in sympathetic ganglia and nerve trunks of rats. Effects of neuronal activity and inositol analogs on [ $^{32}\text{P}$ ]-labelling, synaptic transmission and axonal conduction. *J. Neurochem.* 20: 783-798.
38. White, G.L., H.U. Schellhase, and J.N. Hawthorne. 1974. Phosphoinositide metabolism in rat superior cervical ganglion, vagus, and phrenic nerves: Effect of electrical stimulation and various blocking agents. *J. Neurochem.* 22: 149-158.
39. Yagihara, Y. and J.N. Hawthorne. 1972. Effects of acetylcholine on the incorporation of [ $^{32}\text{P}$ ] orthophosphate *in vitro* into the phospholipids of nerve-ending particles from guinea pig brain. *J. Neurochem.* 19: 355-367.
40. Yamamuchi, L. and P.N. Patil. 1973. Relative potency of cholinomimetic drugs on the bovine iris sphincter strips. *Invest. Ophthalm.* 12: 80-82.
41. Yamamura, H.I. and S.H. Snyder. 1974. Muscarinic cholinergic receptor binding in the longitudinal muscle of guinea-pig ileum with [ $^3\text{H}$ ] quinuclidinylbenzilate. *Mol. Pharm.* 10: 861-867.
42. Yamamura, H.I. and S.H. Snyder. 1974. Muscarinic cholinergic binding in rat brain. *Proc. Natl. Acad. Sci. USA* 71: 1725-1729.